THE ASTROPHYSICAL JOURNAL, 535:90–103, 2000 May 20
© 2000. The American Astronomical Society. All rights reserved. Printed in U.S.A.

SELF-LENSING MODELS OF THE LARGE MAGELLANIC CLOUD

G. GYUK, N. DALAL, AND K. GRIEST
Physics Department, University of California, San Diego, San Diego, CA 92093
Received 1999 September 9; accepted 2000 January 14

ABSTRACT

All of the proposed explanations for the microlensing events observed toward the LMC have difficulties. One of these proposed explanations, LMC self-lensing, which invokes ordinary LMC stars as the long sought-after lenses, has recently gained considerable popularity as a possible solution to the microlensing conundrum. In this paper, we carefully examine the full range of LMC self-lensing models, including for the first time the contribution of the LMC bar in both sources and lenses. In particular, we review the pertinent observations made of the LMC and show how these observations place limits on such self-lensing models. We find that, given current observational constraints, *no* purely LMC disk models are capable of producing optical depths as large as that reported in the MACHO collaboration 2 year analysis. We also introduce a new quantitative measure of the central concentration of the microlensing events and show that it discriminates well between disk/bar self-lensing and halo microlensing. Besides pure disk/bar, we also consider alternative geometries and present a framework which encompasses the previous studies of LMC self-lensing. We discuss which model parameters need to be pushed in order for such models to succeed. For example, like previous workers, we find that an LMC halo geometry may be able to explain the observed events. However, since *all* known LMC tracer stellar populations exhibit disklike kinematics, such models will have difficulty being reconciled with observations. For SMC self-lensing, we find predicted optical depths differing from previous results, but more than sufficient to explain all observed SMC microlensing. In contrast, for the LMC we find a self-lensing optical depth contribution between 0.47×10^{-8} and 7.84×10^{-8}, with 2.44×10^{-8} being the value for the set of LMC parameters most consistent with current observations.

Subject headings: dark matter — galaxies: halos — galaxies: kinematics and dynamics — gravitational lensing — Magellanic Clouds

1. INTRODUCTION

Gravitational microlensing has become a powerful tool for the discovery, limiting, and characterization of populations of dark (and luminous) objects in the vicinity of the Milky Way (MW). Of great interest is the interpretation of the handful of events discovered toward the Magellanic Clouds. If these events are due to a population of objects in an extended MW halo, they can be interpreted to represent between 20% and 100% of the dark matter in our Galaxy (Alcock et al. 1997a; Gates, Gyuk, & Turner 1996). However, the most probable masses of these objects lie in the 0.1–1 $M_\odot$ mass (Alcock et al. 1997a). Such a large number of objects in this mass range is quite problematic (e.g., Fields, Freese, & Graff 1998). Therefore, alternatives to MW halo lensing have been sought to explain the LMC microlensing events.

One alternative, proposed by Sahu (1994a) and Wu (1994), suggests that stars within the LMC itself, lensing other LMC stars, could produce the observed optical depth. This claim has been disputed by several other groups (Gould 1995; Alcock et al. 1997a), who claim that the rate of LMC self-lensing is far too low to account for the observed rate. It was hoped that observation along a different line of sight (i.e., toward the SMC) would resolve this issue. After 5 years of monitoring, there have been two observed microlensing events toward the SMC. The more recent SMC event was a resolved binary lens event (Alcock et al. 1998), allowing determination of the lens distance (Alcock et al. 1998; Afonso et al. 1998; Albrow et al. 1998). The lens was found to lie, with high probability, in the SMC and not in the MW halo. There is also evidence that the only other SMC microlensing event (Alcock et al. 1997c) may reside in the SMC (Palanque-Delabrouille et al. 1998). Thus, all of the relevant lenses whose distances are known are thought to reside in the Magellanic Clouds. This has been interpreted by some as settling the case in favor of the LMC/LMC self-lensing interpretation of the LMC events. This conclusion is not well founded if based solely on the SMC events. The reason, as we discuss below, is fairly simple: the SMC is known to be extended along the line of sight, while there is little evidence that the LMC is similarly extended. In fact, the observations imply that the LMC is distributed as a thin disk, quite unlike its smaller sibling. Thus, unfortunately, the SMC microlensing events do not settle the question of the interpretation of the LMC events, and the controversy remains.

The purpose of this paper is to provide a set of calculations of LMC microlensing that treats LMC self-lensing in a systematic, thorough, and realistic fashion including contributions of both disk and bar. We also provide a convenient set of scaling relations to allow direct estimation of optical depths without repeating our extensive Monte Carlo calculations. We relate the known LMC observations to microlensing predictions and provide a framework within which future observations will easily translate into microlensing predictions. We hope this will serve as a general basis for comparison between observation and theory in the future.

Overall, we find that self-lensing models typically suffer two major defects. First, it is quite difficult for such models to produce enough lensing to account for the observed optical depth while remaining within the bounds set by observation. Second, the optical depth due to disk or bar self-lensing is strongly concentrated on the sky, in contrast

to the relatively uniform distribution of events seen to date. As we discuss below, this can be seen clearly with our newly introduced concentration statistic, $\tilde{\theta}$. These two statements have a major caveat: if the LMC lenses are distributed in an extended or halo-like geometry, it is possible to produce the required optical depth, and the central concentration of the predicted events is significantly diminished. Such an extended or halo-like distribution, however, requires either a hitherto undetected stellar population or a dark MACHO component to the LMC halo. If a dark LMC halo is invoked, then one might expect it to have a similar fraction of dark MACHOs as the MW halo. Otherwise, the presence of such a component in the LMC but not in the Galactic halo would be puzzling. On the other hand, if a stellar LMC halo with a luminosity function similar to the disk is invoked, direct observation of these LMC halo stars should be presently possible. Indeed, as we discuss below, several stellar populations which correspond to stars that do trace the spheroid in our Galaxy have been observed in the LMC, and *all* of them fail to exhibit a halo geometry. Therefore, current observations suggest that the number of stars in any such stellar halo is small and that an LMC stellar halo probably does not greatly contribute to microlensing.

2. MICROLENSING

The first and main reason that previous work has produced such discordant results is that different papers have treated the LMC differently. For example, Gould (1995) and Alcock et al. (1997a) treated the LMC as a thin exponential disk, while Sahu (1994a) and Aubourg et al. (1999) modeled the LMC as being much more extended along the line of sight. These two qualitatively different prescriptions give wildly different predictions for the optical depth and rate of self-lensing. The reason for this is simple. The rate of microlensing is proportional to the Einstein radius of the lens, which is given by

$$R_{\rm E} = \left[2R_{\rm S} \frac{D_{\rm OL} D_{\rm LS}}{D_{\rm OS}} \right]^{1/2} ,$$

where $R_{\rm S}$ is the Schwarzschild radius of the lens, $D_{\rm OL}$ is the angular diameter distance between the observer and lens, $D_{\rm LS}$ is the distance between the lens and source, and $D_{\rm OS}$ is the distance between observer and source. The Einstein radius (and thus the microlensing rate) tends to zero as the lens and source approach each other. In the language of Griest (1991), the "Einstein tube" pinches off at the ends. Therefore, if the lenses are confined to a thin plane along with the sources, the microlensing rate must be small. On the other hand, if the lenses are allowed to move away from the sources, the rate increases. This principle is clearly demonstrated in the SMC. Because of its interactions with the LMC and the MW, the SMC is being tidally disrupted and is consequently quite elongated along the line of sight to the MW (Caldwell & Coulson 1986; Welch et al. 1987). This allows stars within the SMC to be along the same line of sight to us but separated from each other. Consequently, we expect appreciable self-lensing within the SMC, and this expectation is borne out by the large observed SMC self-lensing rate (Alcock et al. 1997c; Palanque-Delabrouille et al. 1998). Indeed, EROS II reports an observed SMC optical depth of $\sim 3.3 \times 10^{-7}$ (Palanque-Delabrouille et al. 1998), and employing the simple model Palanque-Delabrouille et al. used to describe the SMC disk but placing the SMC at 60 kpc, we find predicted self-lensing optical depths of 1.5, 3.0, and 4.4×10^{-7} for an SMC mass of times $10^9\ M_\odot$ and SMC vertical scale heights of 2.5, 5.0, and 7.5 kpc, respectively. (We note that these numbers do not agree with the optical depths that Palanque-Delabrouille et al. predicted.)

To answer the question of whether LMC self-lensing is significant, we must understand the distribution of stars within the LMC. If the LMC is a thin disk, then the small rates and optical depths derived by Gould and others will be valid. Conversely, if the LMC is puffy, then the large rates and optical depths claimed by Sahu and others will be correct. The basis for any description of the LMC is the set of observations that have been made of the LMC. We therefore turn to the current state of observations of the LMC.

3. OBSERVATIONS AND MODELS OF THE LMC

3.1. *LMC Disk*

Since the pioneering work of de Vaucouleurs (1957), it has been well accepted that the stellar component of the LMC has an exponential profile. The value de Vaucouleurs measured for the exponential scale length, R_d, continues to agree with the current value of 1.°8 (Alcock et al. 2000b), which corresponds to a physical scale length of 1.6 kpc for a distance to the LMC of 50 kpc. In addition to this stellar population, the LMC possesses significant quantities of H I gas, which has recently been mapped out by Kim et al. (1998). Their images show clear spiral structure in the gas, supporting the notion that the LMC is a typical dwarf spiral galaxy. The gas is confined to a thin disk, inclined at roughly 30°, with a position angle $\sim 170°$. See Westerlund (1997, p. 30) for a compilation of various estimates of the LMC orientation as well as Kim et al. (1998) for a recent value. Based on these observations, in this paper we describe the stellar disk by a double exponential profile, given by

$$\rho_d = \frac{M_{\rm disk}}{4\pi z_d R_d^2}\, e^{-(R/R_d) - |z/z_d|} ,$$

where R_d is the radial scale length, z_d is the vertical scale height, and $M_{\rm disk}$ is the disk mass. Note that R_d is well constrained by observation, but we have some leeway in the scale height and in the mass of the disk. We discuss these two quantities in more detail later. The disk is inclined at angle i to our line of sight and has position angle P.A.

3.2. *LMC Bar*

As is well known, the LMC hosts a prominent bar of size roughly $3° \times 1°$. The bar has the unusual (although not unique, e.g., Freeman 1996; Odewahn 1996) property of being offset from the dynamical center of the H I gas. The offset is $\approx 1.°2$ (Westerlund 1997), corresponding to a physical offset of ~ 1 kpc. The kinematics of the LMC bar are consistent with solid-body rotation (Odewahn 1996), as is seen in numerous barred galaxies. The distribution of matter within the bar is not well known. Measurements of the luminosity function, after subtraction of disk light, show it to be consistent with an exponential profile along the major axis (Bothun & Thompson 1988; Odewahn 1996). This is consistent with certain other bars, which can be well described by an exponential along the major axis and a Gaussian profile along the minor axis (Blackman 1983; Ohta 1996). For our own Galactic bar, Dwek et al. (1995)

have proposed a profile similar to a Gaussian, but more boxy, and this form is also consistent with bars in certain other galaxies.

Thus, unlike the disk, the bar is not particularly well defined. With little guidance from observations, we have treated the bar simply as a triaxial Gaussian, with axis ratios chosen to match the observed ratios. We let

$$\rho_b = \frac{M_{\rm bar}}{(2\pi)^{3/2} x_b\, y_b\, z_b}\, e^{-(1/2)[(x/x_b)^2 + (y/y_b)^2 + (z/z_b)^2]},$$

where x, y, z are coordinates along the principal axes of the bar, and x_b, y_b, z_b are the scale lengths along the three axes. The value of $M_{\rm bar}$ is the total mass of the bar. This form is somewhat similar to models used to describe other galactic bars (e.g., Dwek et al. 1995). We place the bar in the same plane as the disk; however, we place the bar center at the position of the observed bar centroid, at ($\alpha = 5^{\rm h}24^{\rm m}$, $\delta = -69°48'$) (de Vaucouleurs 1957). We use a position angle for the bar of 120°.

It is not clear, at this point, how great an influence the bar exerts over the dynamics of the surrounding gas and stars. In many barred galaxies, the bars sweep up gas and drive it toward the center (Kenney 1996; Ho et al. 1996; Sakamoto et al. 1999). In our own Galaxy, the kinematics of gas in the inner regions is strongly influenced by the putative bar (Weiner & Sellwood 1999). While there is evidence for nonaxisymmetric flows in the vicinity of the bar (Dottori et al. 1996; Odewahn 1996), indicating that the bar may be dynamically important, the H I maps of Kim et al. show that the LMC bar does not dominate the central dynamics. From this we conclude that the mass of the bar cannot exceed the disk mass in the central regions, which leads us to a bound on the bar mass. Now, ~25% of the disk mass lies within 1 scale length, while most of the bar lies in this same central region. We thus arrive at the following restriction: $M_b < 25\% M_d$ to avoid bar domination. This agrees nicely with the estimates of Sahu (1994b), who suggested a bar-to-disk mass ratio in the range 15%–20% based on luminosity considerations.

3.3. *LMC Velocity Distribution and Vertical Scale Height*

Now we turn to the velocity distribution of the model stars. Perhaps the best determination of the inner velocity curve of the LMC is in the work of Kim et al. (1998). When supplemented by outer rotation curves derived from carbon stars (Kunkel et al. 1997) and clusters and planetary nebulae (PNs) (Schommer et al. 1992), the basic outline is clear: the circular velocity rises rapidly in the first 2 kpc and then levels off and is flat at about 70 km s^{-1} out to at least 8 kpc. There are indications of a possible dip at 3 kpc, although this may not be significant. For our models we approximate the rotation curve by solid-body rotation out to a radius $r_{\rm solid} = 2$ kpc, followed by flat rotation at $v_c = 70$ km s^{-1}.

These studies help to define to bulk motions of gas and stars in the LMC. However, as Gould (1995) has shown, velocity dispersions (and the implied scale heights) are crucial in determining the optical depth and rate of microlensing. So let us consider measurements of the velocity dispersion of LMC populations. Prevot, Rousseau, & Martin (1989) studied late-type supergiants and H II regions, concluding that the internal velocity dispersion of this population is approximately 6 km s^{-1}. This is quite close to that of the H I gas, 5.4 km s^{-1} (Hughes, Wood, & Reid 1991), which is hardly surprising as these tracers all belong to a very young population. A somewhat older population is probably illustrated by the disklike ($\sigma_v \sim 10$ km s^{-1}) CH stars found by Cowley & Hartwick (1991) which seem to correspond to "CH-like" stars found in the Galactic disk (Yamashita 1975).[1] Cowley & Hartwick also found, however, a population with a considerably higher velocity dispersion (20–25 km s^{-1}) that presumably corresponds to an even older population. Meatheringham et al. (1988), in a study of PNs, found that the intermediate population of stars represented by the PNs are rotating as fast as and in the same disk as the gas, but with a velocity dispersion of 19.1 km s^{-1}. Bessel, Freeman, & Wood (1986) observed old long-period variables (OLPVs), which the authors contend trace the oldest stellar populations, and obtained a mean line-of-sight velocity dispersion of about 30 km s^{-1}. Hughes et al. (1991) also observed OLPVs and obtained similar results ($\sigma \sim 30$ km s^{-1}). We note here, for future reference, that a spheroidal distribution would require velocity dispersions of $\sigma \approx v_c/\sqrt{2} \approx 50$ km s^{-1}. Since the observed dispersions of the OLPVs fall far short of this, we see that even this oldest population derives much of its support from rotation and therefore exhibits "disklike" kinematics.

The general trend among the many kinematic studies of the LMC seems to be clear: tracers have velocity dispersions ranging from ~5 km s^{-1} for very young ages to ~30 km s^{-1} for the most ancient populations. *All* LMC populations studied to date have disklike kinematics regardless of age (Olszewski, Suntzeff, & Mateo 1996). Table 1 lists some of the more recent kinematic studies of the LMC by population type, velocity dispersion, and probable age.

From the velocity dispersions, let us now turn to the vertical scale heights. Bessel et al. (1986) estimated the vertical scale height of the oldest population to be roughly 0.3 kpc, while Hughes et al. (1991) estimated the scale height to be $\lesssim$0.8 kpc. They emphasized that this was the oldest population, accounting for at most 2% of the mass of the LMC. The majority of the LMC disk, they contend, should possess a more compact vertical distribution and smaller vertical velocity dispersions. This is supported by RR Lyrae and cluster studies which suggest that the ancient extended populations make up considerably less than 10% of the LMC stars (Olszewski et al. 1996; Kinman et al. 1991). We thus allow our scale height (which should characterize the bulk of the LMC population) to range up to 0.5 kpc and adopt velocity dispersions in a corresponding range of 10–30 km s^{-1}. In theory, these parameters should be tied together by the vertical Jeans equation (however, see Weinberg 1999). In practice, our knowledge of the total mass and mass distribution of the LMC is poor enough that we simply note that the opposite extremes of these ranges (i.e., 10 km s^{-1} with 0.5 kpc and 30 km s^{-1} with <0.2 kpc) are likely inconsistent.

3.4. *LMC Halos: Light and Dark*

The above distributions describe the known stellar populations. We again reiterate that the nondetection of any

[1] One should be cautious in identifying CH stars and Galactic CH stars. The appearance of carbon is a complex and largely unknown function of both age and metallicity, so LMC carbon stars might differ from their galactic siblings.

TABLE 1

OBSERVED VELOCITY DISPERSIONS FOR VARIOUS POPULATIONS

Population	Reference	Velocity Dispersion	Age
Supergiants	1	6	Young
H II	1	6	Young
H I	2	5.4	Young
VRC	3	18.4	Young?
PNs	4	19.1	Intermediate
OLPV	2	33	Old
ILPV	2	25	Intermediate
YLPV	2	12–15	Young
OLPV	5	30	Old
Metal-poor giants	6	23–29	Old
Metal-rich giants	6	16.0	Intermediate?
New clusters	7	20	Intermediate
Old clusters	7	30	Old
Carbon stars	8	15	Young
CH stars (disk)	9	10	Young/intermediate?
CH stars (halo)	9	20–25	Old

REFERENCES.—(1) Prevot et al. 1989; (2) Hughes et al. 1991; (3) Zaritsky & Lin 1997; (4) Meatheringham et al. 1988; (5) Bessel et al. 1986; (6) Olszewski 1993; (7) Schommer et al. 1992; (8) Kunkel et al. 1997; (9) Cowley & Hartwick 1991.

stellar halo population ($\sigma_v \sim 50$ km s^{-1}) places severe constraints upon the existence of such a stellar halo. The above-noted RR Lyrae and cluster studies, along with the OLPV observations, limit the stellar halo to perhaps 5% of the mass of the LMC (Hughes et al. 1991; Olszewski 1993; Olszewski et al. 1996; Kinman et al. 1991).

This, however, places no limits upon the existence of a dark halo, to which we now turn. Obviously, even less is known about the LMC dark matter than its luminous populations. As Kim et al. (1998) discuss, the observed LMC rotation curve is inconsistent with the distribution of known populations, given the assumption of a *constant* mass-to-light ratio. Schommer et al. (1992) obtain similar results. Although the variation in the mass-to-light ratio required to explain the rotation curve with luminous matter alone is less than a factor of 2, we can take these results as weak evidence for dark matter within the LMC. This should not be too surprising, since studies of the velocity curves of similar dwarf galaxies show that they are dominated by dark matter (see, e.g., Carignan & Purton 1998). Models without dark halos also exist that can explain the rotation curves (D. Alves 1999, private communication), but these will not be discussed here. There are numerous models that have been used to describe dark matter in galaxies. Most common, and perhaps easiest, is the simple spherical pseudoisothermal distribution,

$$\rho_h = \rho_0 \left(1 + \frac{r^2}{a_h^2}\right)^{-1},$$

with core radius a_h and central density ρ_0. In the limit $a_h \to 0$, this distribution gives an isothermal Maxwellian velocity profile (Binney & Tremaine 1987). For the LMC, however, core radii smaller than $a_h \sim 1$ kpc lead to problems matching the rotation curve. Although not self-consistent, for simplicity we use $a_h > 1$ kpc and a uniform Maxwellian velocity distribution. We take the fraction of this halo in MACHOs to be f_M.

Since the LMC is embedded in the (dominating) gravitational potential of our Galaxy, we expect the LMC to have a tidal radius beyond which objects are not stably bound to the LMC (Binney & Tremaine 1987). This places a limit on the size of the LMC halo. Although the density should smoothly decline to zero near the tidal radius, for simplicity we instead implement a truncation radius, r_t, beyond which the LMC halo density abruptly vanishes. Using star counts from the 2MASS survey, Weinberg (1998) has estimated $r_t \approx 11$ kpc. This is the value we adopt.

3.5. *LMC Mass*

The question of the LMC mass is an unsettled one. A few of the more recent mass estimations are shown in Table 2. Estimates range from only a few times $10^9\ M_\odot$ to $\sim 2 \times 10^{10}\ M_\odot$. Close inspection, however, reveals a few regularities. The highest estimates are based on the spheroidal estimator of Bahcall & Tremaine (1981), which assumes both velocity isotropy and a spherical mass distribution. Since both of these conditions are likely to be violated, the spheroidal estimators should be taken as upper limits. A similar argument can be made for the point mass estimation of Kunkel et al. (1997). With these caveats in mind, the data seem consistent with a disk of perhaps $3 \times 10^9\ M_\odot$ and a halo whose mass within 8 kpc is roughly $6 \times 10^9\ M_\odot$. While the extremely high-quality H I data of Kim et al. (1998) would appear to rule out a disk mass much in excess of this, the halo component is much more uncertain. We thus take $M_{\rm disk} + M_{\rm bar} \leq 5.0 \times 10^9\ M_\odot$ and allow the total LMC halo mass within 8 kpc to range up to $1.5 \times 10^{10}\ M_\odot$. In Figure 1 we show the rotation curves associated with several choices of component masses. While our preferred parameters fit the observed velocity profile quite nicely, the upper ends of our allowed ranges are clearly starting to run afoul of the observations.

This covers all of the populations we consider for LMC self-lensing. The various parameters and their preferred values are listed in Table 3. However, since observations are subject to change, it is worthwhile to consider not only the currently preferred description of the LMC, but a wide class of models and parameters, so that future observations easily translate into microlensing predictions. We have therefore also indicated the acceptable range of each model parameter in Table 3. Of course, models that simultaneously take

TABLE 2

ESTIMATES OF THE LMC MASS

Study	Mass Estimate ($M_\odot$)	Radius (kpc)	Component	Estimation Type
1.....	6.0×10^9	4.5	Total	Spheroidal estimator
2.....	2.5×10^9		Disk	Rotation curve fit
	3.4×10^9	8	Halo	
3.....	$\sim 2.0 \times 10^{10}$	5	Total	Spheroidal estimator
	1.0×10^{10}	8	Total	Rotation estimate
4.....	3.2×10^9		Disk	Rotation maximum fit
	6.0×10^9	5	Total	
5.....	6.2×10^9	5	Total	Point mass estimation
	$< 1.0 \times 10^{10}$		Total	

NOTE.—Some entries refer to specific components, such as the disk or halo, while other entries correspond to the LMC as a whole.

REFERENCES.—(1) Hughes et al. 1991; (2) Kim et al. 1998; (3) Schommer et al. 1992; (4) Meatheringham et al. 1988; (5) Kunkel et al. 1997.

extreme values of all the parameters may not be realistic. While this range *spans* the set of acceptable models, not all models in this range are acceptable.

4. CALCULATIONS

Using the models specified in the previous section, the microlensing event rate, optical depth, and timescale distribution can be calculated. The microlensing rate is the number of events per year per star. To obtain the total number of events expected for an experiment one would multiply the rate by the observational exposure, which is defined as the number of monitored stars times length of time they were monitored. The optical depth is the probability that a given source star is lensed with a magnification greater than 1.34.

The optical depth along a given line of sight is given by

$$\tau = \frac{1}{N_s} \int_0^\infty dL n_s(L) \int_0^L dl \pi R_E^2(L, l) n_l(l) ,$$

where n_s is the number density of sources, n_l is the number density of lenses, R_E is the Einstein radius defined above, $L = D_{OS}$ is the distance to the source, and $N_s = \int n_s dL$ is the total number of sources along the line of sight. Writing $\rho(x) = \langle m \rangle n_l(x)$ and inserting the expression for the Einstein radius R_E gives

$$\tau = \frac{4\pi G}{c^2 N_s} \int_0^\infty dL n_s(L) \int_0^L dl \frac{l(L-l)}{L} \rho_l(l) .$$

TABLE 3

MODEL PARAMETERS

Parameter	Preferred Value	Allowed Range
Inclination (deg).....	30	20–45
R_d (deg)	1.8	1.8
z_d (kpc)	0.3	0.1–0.5
v_c (km s^{-1})	70	60–80
L (kpc)	50	45–55
σ_v (km s^{-1})	20	10–30
a_h (kpc).....	2	1–5
M_{d+b}(8 kpc) ($M_\odot$).....	3×10^9	$< 5 \times 10^9$
M_{dark}(8 kpc) ($M_\odot$).....	6×10^9	$< 1.5 \times 10^{10}$
M_{bar}/M_{d+b}	0.15	0.05–0.25
$M_{stellar\ halo}$ ($M_\odot$).....	0×10^8	$0–5.0 \times 10^8$

NOTE.—$M_{d+b} = M_{disk} + M_{bar}$. All masses are for LMC distances of 50 kpc.

Before proceeding further, we discuss the source distribution in more detail. In the simplest approach the source density would be set to the mass density (disk + bar) we have already discussed. This ignores two important issues. First, the LMC is seen almost face-on, and hence the thin dust and gas disk obscures the far half of the stars. This preferentially removes source stars with the highest optical depth, lowering the observed optical depth. Modeling the extinction as a zero-thickness plane of 0.4 V magnitudes (Oestreicher & Schmidt-Kaler 1996), a rough approximation shows that the effect should reduce the optical depth by about 15% for disk-disk self-lensing. In the following, we ignore this effect, simply noting that our quoted results are overestimates. The second issue concerns the differing populations of the disk and bar. These different populations (due to the varying ages and star formation history) yield different numbers of sources per unit mass in the disk and bar. Unfortunately, with the present knowledge of the bar and disk luminosity functions and relative metallicities, etc., a precise calculation is impossible. We therefore assume a uniform mass-to-source ratio. A third potential cause for concern is blending. However, detailed simulations by the MACHO collaboration (Alcock et al. 2000c) indicate that this is not in fact a severe problem.

We have found it convenient to calculate the optical depth, event rate, and duration distribution using a Monte Carlo method. One advantage of the Monte Carlo technique is that it easily allows consideration of arbitrary spatial distributions of lenses and sources. Another important advantage of the Monte Carlo method is the ease with which we were able to average over the experimental fields as discussed in the following section. In addition, the separate integrals for the optical depth, rate, and event timescales can all be evaluated simultaneously, in one fell swoop.

4.1. *MACHO Fields*

For self-lensing models, the optical depth varies rapidly with position in the LMC. Thus, a single number, "the optical depth to the LMC," is useful only if the precise location of the observed sources is specified. In order to make the comparison to the observed optical depth, we have chosen to average our results over the MACHO collaboration fields (Alcock et al. 1997a). Ideally we should fold in the experimental efficiency and relative source numbers in each field as observed. Since these numbers are

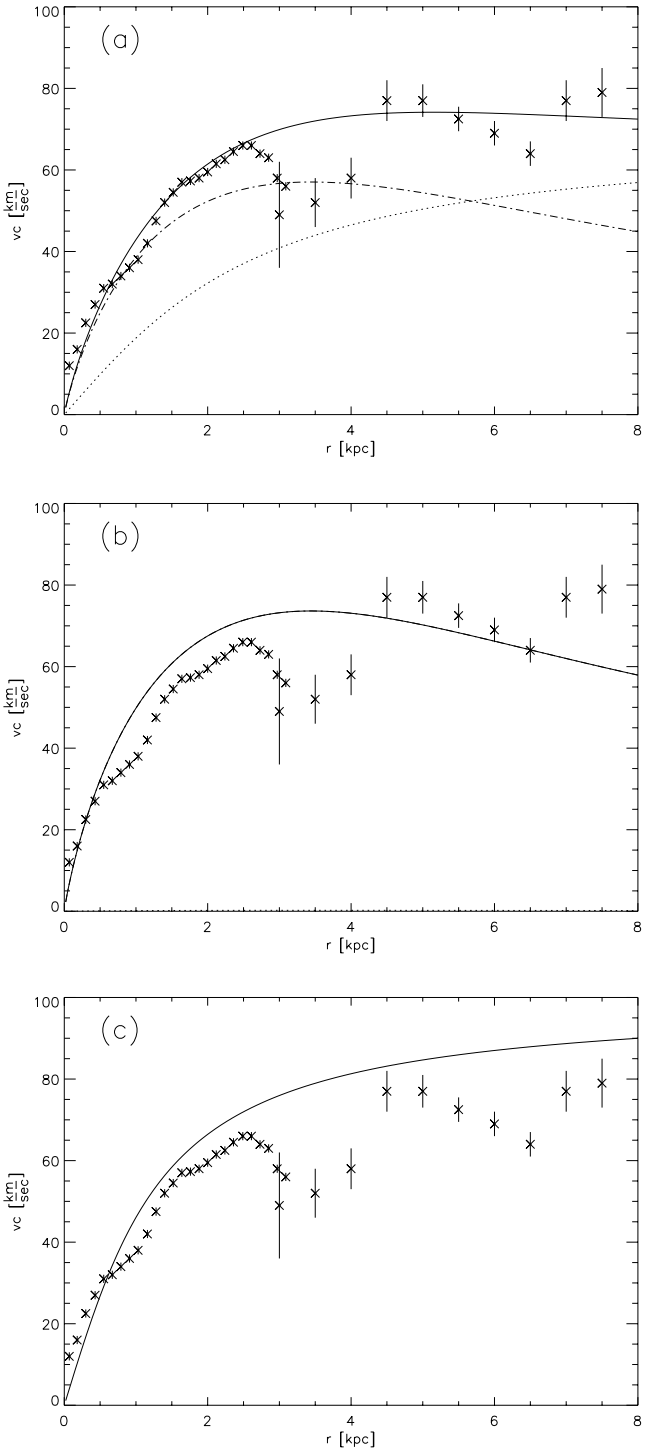

FIG. 1.—Model rotation curves. The plotted points with error bars are from Kim et al. (1998) and Kunkel et al. (1997). (*a*) Predicted rotation curve for our preferred model, with $M_{\rm disk} = 3 \times 10^9\ M_\odot$ (entirely in the double exponential disk), $M_{\rm dark}(8\ {\rm kpc}) = 6 \times 10^9\ M_\odot$, and $a_h = 2.0$ kpc. The dash-dotted line shows the disk contribution, and the dotted line shows the halo contribution. (*b*) Predicted rotation curve for the maximal disk we allow, $M_{\rm disk} = 5 \times 10^9\ M_\odot$. Note that it already significantly overshoots the observed velocities. Any additional dark component exacerbates the problem. (*c*) Curve for the maximum dark halo mass, $M_{\rm dark}(8\ {\rm kpc}) = 1.5 \times 10^{10}\ M_\odot$, and $a_h = 1$ kpc. Clearly, masses in excess of this can safely be ruled out.

unavailable, however, we have weighted each field by the *model* number of stars. We show in Figure 2 the fields over which the optical depth is averaged. The solid outlines depict the 22 fields covering about 10 deg^2 used in the MACHO year 2 analysis (Alcock et al. 1997a). Note that the year 2 fields are concentrated along the regions of highest numbers of source stars. The dotted outlines describe the roughly 40 deg^2 (82 fields) that are being monitored by the MACHO collaboration.[2] These cover most of the LMC disk out to a radius of 3°.5 from the center (about 2 disk scale lengths). Later we will discuss possible observational consequences of the increased coverage. Also of interest are the 30 fields that are presented in the MACHO collaboration 5.7 year analysis (Alcock et al. 2000a). We note that the EROS II collaboration is similarly observing 66 deg^2 of the LMC disk (Lasserre et al. 1999), while the OGLE II collaboration monitors 4.2 deg^2 (Udalski, Kubiak, & Szymanski 1997).

4.2. *Mass Function*

Although the optical depth is independent of the mass function, the event rate and the timescale distribution do depend upon the lens masses. We therefore must consider an appropriate mass function for the lensing population. As we expect the rate to be dominated by low-mass stars, we choose to employ the mass function derived by Gould, Bahcall, & Flynn (1997), which they based upon counts of M dwarfs in the MW disk. Gould et al. found that

$$\frac{dN}{dm} \propto \left(\frac{M}{0.59\ M_\odot}\right)^\alpha ,$$

with $\alpha \approx -0.56$ for $m < 0.59\ M_\odot$ and $\alpha \approx -2.21$ for

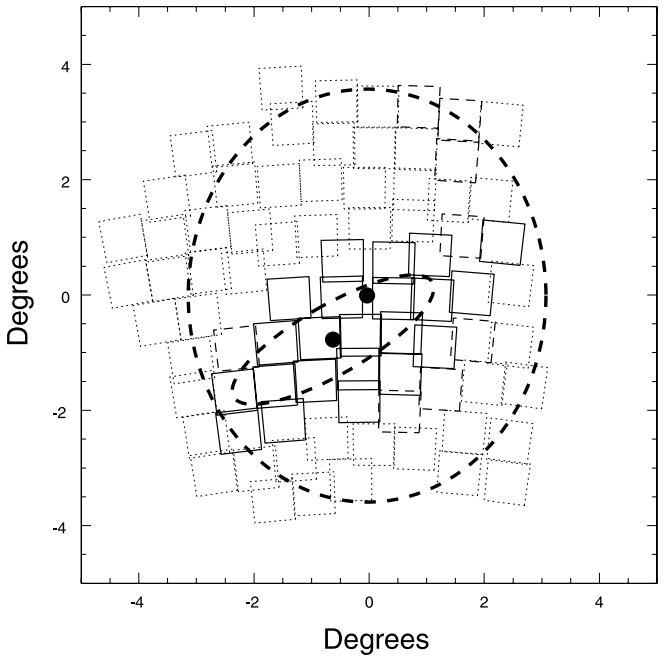

FIG. 2.—MACHO fields. The solid outline squares depict the 22 MACHO fields reported in Alcock et al. (1997a). The dashed squares are the eight additional fields MACHO will report in their year 5 paper, and the dotted squares are the other 52 fields that they monitor. The thick-dashed ellipses show the position and orientation of our model disk and bar. They are plotted at 2 scale lengths.

[2] The centers of all 82 fields can be accessed from the MACHO collaboration website at http://wwwmacho.mcmaster.ca/.

$m > 0.59\ M_\odot$. Since the timescales and rate are dependent only on the square root of the masses, the precise details of the LMC mass function are not important unless it is radically different from that of the MW.

5. RESULTS

The measured total optical depth toward the LMC from the 2 year MACHO collaboration analysis is $2.9^{+1.4}_{-0.9} \times 10^{-7}$ (Alcock et al. 1997a). How does this compare with the predicted range of optical depths of the above models?

5.1. *Disk/Bar Optical Depth and Scalings*

Let us first consider disk-disk lensing. Evaluating the integral and plugging in the preferred disk parameters listed in Table 3, we obtain a (22) field-averaged optical depth of $\tau = 1.46 \times 10^{-8}$ for disk-disk lensing. This is the best value for the disk-disk optical depth, given the current status of observations. As noted, however, we should explore the dependence of τ upon the model parameters. We can obtain a reasonable scaling using a simpleminded argument. Let us first consider the optical depth for a single source star at the LMC center. This integral is easy to do exactly, but for our purposes we are interested in its asymptotic behavior. Writing the integral in dimensionless form, we see it is approximately $\propto \rho_0 \int e^{-Ax} x\, dx \propto \rho_0 A^{-2}$, where $\rho_0 = M_{\rm disk}/(4\pi R_d^2 z_d)$ is the central density and

$$A = L\left(\frac{\cos i}{z_d} + \frac{\sin i}{R_d}\right)$$

is the only other form in which these parameters enter the integral. The extended source distribution will modify this scaling, but for disk-disk lensing, the source distribution enters the line-of-sight integral again in the form of A. Thus, $\tau \sim \rho_0 L^2 F(A)$ should capture the essential behavior of the three-dimensional averaged optical depth, with asymptotic leading behavior $\tau \propto \rho_0 A^{-2}$. For the LMC, $A \approx 160$, so we expect the expansion

$$\tau \propto \frac{M_{\rm disk} L^2}{R_d^2 z_d A^2}\left(1 + a_1 A^{-1} + a_2 A^{-2} + \cdots\right)$$

to describe accurately the scaling of the optical depth with the parameters over the range of interest, even if we keep only the first one or two terms. However, for estimation purposes, the leading behavior will be good enough.

We arrive at an interesting relation if we further approximate this already zeroth-order treatment. For a nearly face-on, thin disk, $A \approx (L \cos i)/z_d$. Then $\tau \propto M z_d/(R_d^2 \cos^2 i)$. Note that a similar result was derived by Sahu & Sahu (1998). Now, quantities such as M, R_d, etc., are derived, not measured directly. They are inferred from measured parameters such as the apparent axis ratio $k = \cos i$, the rotation curve (which itself is derived from radial velocity measurements), the distance L, and the vertical velocity dispersion σ_z. For example, the vertical scale height z_d is typically computed using the Jeans equations, which for a self-gravitating thin disk in equilibrium demand that $z_d \sim \sigma_z^2/\Sigma$, where Σ is the local surface density. Inserting this into our scaling for τ gives

$$\tau \propto \frac{\sigma_z^2}{\cos^2 i}\,.$$

This, of course, is Gould's (1995) analytic result. Gould's point is that for disk-disk lensing, to lowest order, the distance of the LMC and the total mass (rotation curve) are irrelevant; that is, the only directly observed quantities that seem to matter are the velocity dispersion and axis ratio. It is important to keep in mind that this conclusion is predicated upon the validity of the self-gravitating, thin-disk, steady-state solutions to the Jeans equations, which Weinberg (1999) has argued may not be applicable to the LMC. We feel that it is better to base microlensing estimates upon parameters like the scale height that are directly tied to the spatial density distribution rather than quantities like the velocity dispersion, which require questionable assumptions.

The optical depths and expected scalings for the other three cases—bar-disk, bar-bar, disk-bar—can be computed with similar ease. For our preferred set of parameters, we find $\tau_{\rm bd} = 1.25 \times 10^{-8}$, $\tau_{\rm bb} = 1.37 \times 10^{-8}$, $\tau_{\rm db} = 8.7 \times 10^{-9}$ (22 fields). Again, we may also be interested in these optical depths for different parameter values, so let us consider the scaling behavior of these integrals. Now, we previously derived an approximate form by considering the limit of a compact source distribution and diffuse lens distribution. What if we reverse the situation and instead imagine a compact lens distribution and extended source distribution? For definiteness, consider a single lens at the LMC center, lensing background stars with density profile ρ_s. In addition, let ρ_s be strongly peaked about the LMC center. Then the optical depth takes the approximate form $\tau \propto \int dl \rho_s(l) L l/(L + l) \sim L^2 \int \rho_s\, x dx$, the exact same form we derived earlier but with ρ_s replacing ρ_l. This should not be surprising, since in the limit $D_{\rm OS} \approx D_{\rm OL}$, the Einstein radius becomes a function only of $D_{\rm LS}$. Since only the relative distance from source to lens matters, τ becomes (in some sense) symmetric in ρ_s and ρ_l. To sum up, when both the source and lens distributions are compact but the source distribution is more compact, we expect $\tau \propto L^2 \int \rho_l\, x dx$, and when the lens distribution is more compact, then $\tau \propto L^2 \int \rho_s\, x dx$. For true self-lensing (disk-disk or bar-bar) these expressions are identical.

With these ideas in mind, we can now work out the approximate scalings. Let us first consider bar-bar lensing. The dimensionless integral in this case behaves, to leading order, like $\int e^{-Bx^2/2} x\, dx \sim B^{-1}$, where

$$B = L^2\left[\frac{\cos^2 i}{z_b^2} + \sin^2 i\left(\frac{\sin^2 \psi}{x_b^2} + \frac{\cos^2 \psi}{y_b^2}\right)\right]$$

and ψ is related to the bar's position angle on the sky by $\tan(\text{P.A.}_{\rm bar} - \text{P.A.}_{\rm disk}) = \tan \psi \cos i$. Thus, τ scales roughly like

$$\tau \propto \frac{M_{\rm bar} L^2}{x_b y_b z_b B}\,.$$

Now we turn to the cross terms (disk-bar and bar-disk). Clearly, the bar Gaussian distribution is more compact than the disk double exponential distribution, so we expect both of these terms to have the disk scaling.

Figure 3 shows the calculated optical depths averaged over 22 fields as a function of various parameters as well as the predictions from the scaling laws (normalized to match at the preferred parameters). In general the scalings are reasonably accurate. The scalings work about as well for the 30 field set and the 82 field set. For an order of magnitude estimate, one can use pure disk-disk with the subzeroth-

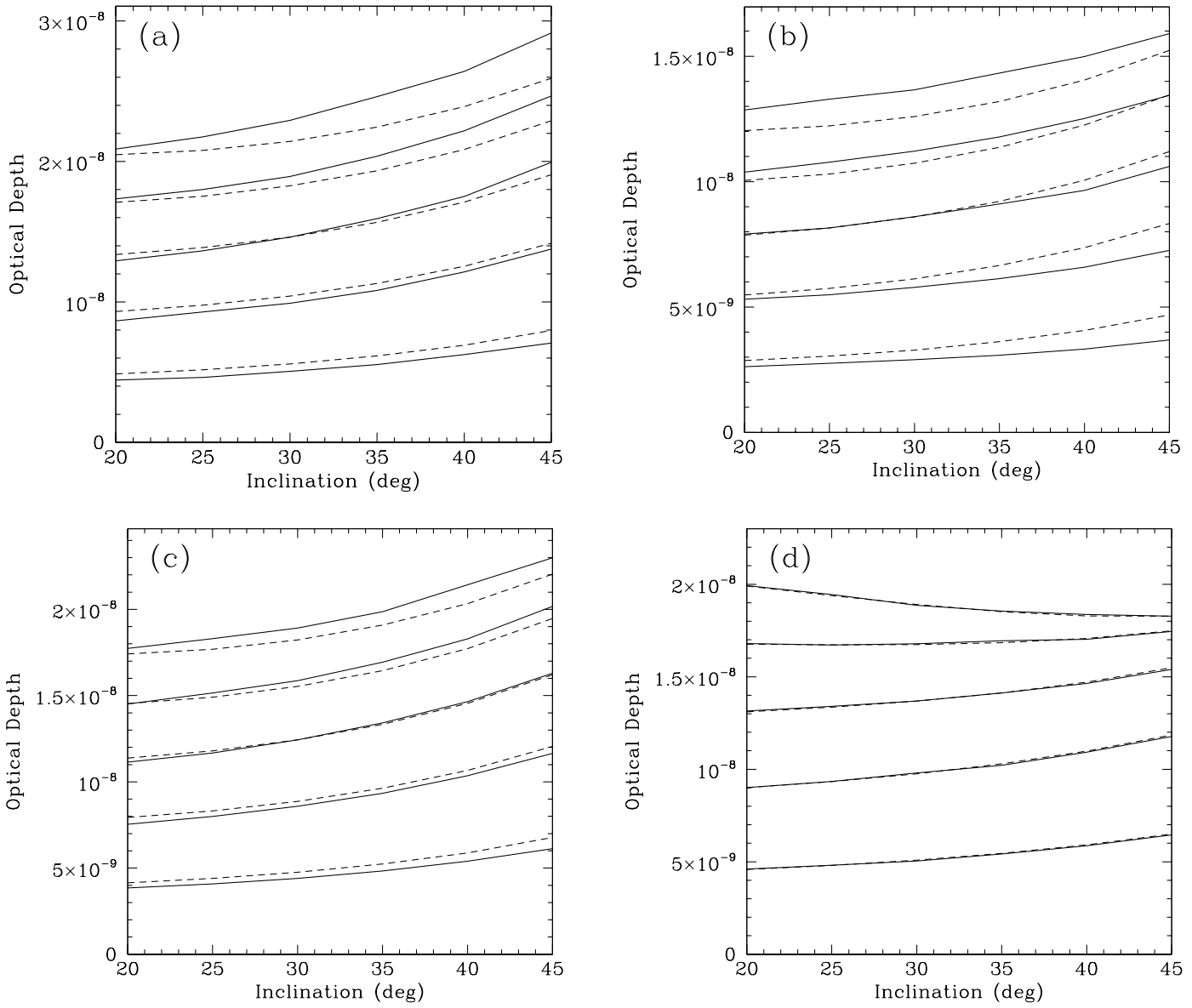

FIG. 3.—Variation of optical depth with model parameters; (*a*) is disk-disk, (*b*) is disk-bar, (*c*) is bar-disk, and (*d*) is bar-bar. The solid lines are the results of our numerical calculation of τ for vertical scale height $z = 0.1, 0.2, 0.3, 0.4, 0.5$, from bottom to top. All other parameters were set to their preferred values. The dashed lines are the predicted values using the scalings described in the text for the same parameters. As expected, the scaling is most accurate for bar-bar, where both the source and lens distributions are compact.

order scaling given above, namely,

$$\tau \approx 1.7 \times 10^{-8} \left(\frac{z_d}{0.3 \text{ kpc}}\right)\left(\frac{M}{3 \times 10^9\ M_\odot}\right) \times \left(\frac{R_d}{1.6 \text{ kpc}}\right)^{-2}\left[\frac{\cos i}{\cos 30^\circ}\right]^{-2}.$$

For the 82 field sample the scaling is the same but the prefactor is 1.05, while for the 30 field sample it is 1.33. A complete average over the LMC disk out to very large radii would give a prefactor of 0.72.

The total optical depth for a particular set of model parameters is somewhat involved to calculate. Since the spatial distribution of the various source populations is different, one cannot simply add together the mass weighted-average optical depths. Instead, one needs to add the optical depths weighted at the field level and then calculate the total optical depth from the field values. No combination of parameters within our ranges allows an optical depth greater than 8.0×10^{-8}. For the preferred values the optical depth is 2.4×10^{-8}. Note that this value is *10 times* smaller than the observed optical depth.

5.2. *Timescales*

Figure 4 shows the timescale distribution for our preferred disk/bar model, using the mass function from Gould et al. (1997). The efficiency weighted-average event duration $\langle \hat{t} \rangle = 101$ days. This is consistent with the observed $\langle \hat{t} \rangle$ of 84 days (Alcock et al. 1997a), given the observational uncertainties and our lack of knowledge of the precise details of the mass function and velocity distribution. This profile is fairly uniform over the face of the LMC.

5.3. *LMC Halo Optical Depth*

We have also calculated the optical depth due to a possible LMC MACHO halo. The optical depth is shown in

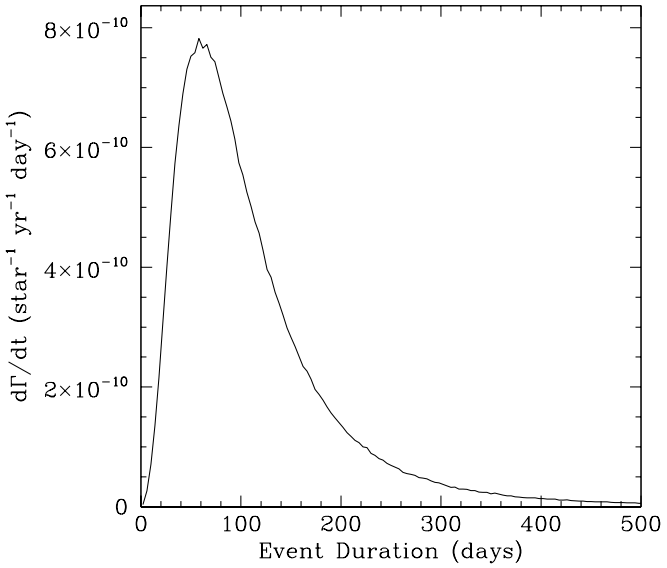

FIG. 4.—Timescale distribution averaged over 22 fields for our preferred model. See text for more details.

Figure 5 as a function of the halo core, a_h. If the mass of the halo is varied the optical depth scales linearly. The values shown are for a $6 \times 10^9\ M_\odot$ LMC halo 100% composed of MACHOs. We find values of the optical depth between $\sim 7.5 \times 10^{-8}$ and $\sim 8.5 \times 10^{-8}$ depending on parameters. It is clear that a halo-type configuration is much more effective at producing optical depth than the disk/bar. Now, there are at least two possible types of LMC halos, both of which could, conceivably, be present simultaneously. First, a dark matter halo, common in dwarf galaxies, is possible. The composition of such a halo should be similar to the composition of the MW halo (i.e., unknown!). If the MW halo has a fraction f_M of MACHOS (the remainder presumably consisting of some exotic nonbaryonic material), then

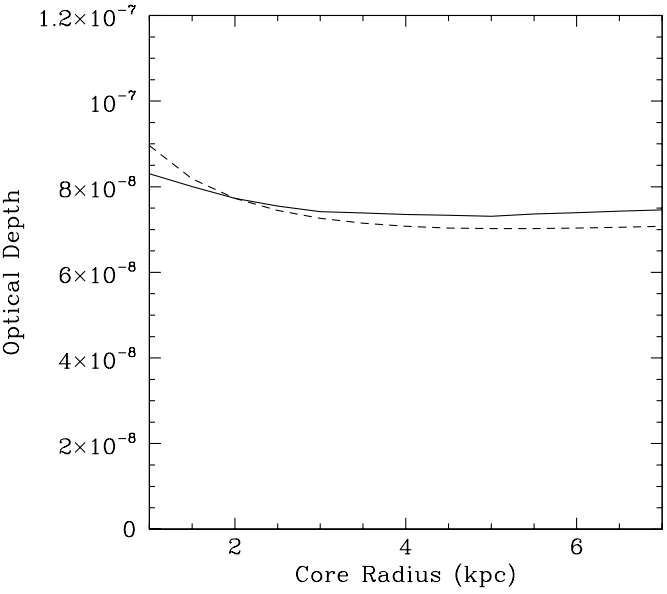

FIG. 5.—Optical depth as a function of halo core radius. The halo is taken to be 100% MACHOs with a mass of $6.0 \times 10^9\ M_\odot$ within 8 kpc. The source distribution is our preferred disk/bar model. Note how insensitive the optical depth is to the core radius. The solid line shows the numerical result, and the dashed line shows the scaling described in the text.

the LMC halo might have a similar fraction. If so, then microlensing of the LMC halo lenses would constitute discovery of dark matter, but the implied halo fraction would depend upon the mass of the LMC halo (Weinberg 1998; Kerins & Evans 1999). That is, the predicted optical depth of the MW halo plus the LMC halo would be roughly $\tau \simeq f_M[4.7 \times 10^{-7} + (0\text{–}2.3) \times 10^{-7}]$, and so the effect of including a dark LMC halo would be to reduce the derived MACHO halo fraction by $\Delta f_M/f_M = -(0\text{–}2.3)/[4.7 + (0\text{–}2.3)] = -(0\%\text{–}33\%)$. Using the current estimate f_M of 50% (Alcock et al. 1997a), inclusion of an LMC halo lowers f_M to somewhere in the range 33%–50%.

The other type of possible LMC halo is a stellar halo with a luminosity function similar to that in the disk. This could consist of stars stripped from the disk (Zaritsky & Lin 1997; Weinberg 1999) or something corresponding to the spheroid of the MW. This is the halo of interest in creating a non–dark matter explanation for LMC microlensing. As discussed above, the mass of such a halo is tightly constrained by numerous observations.

As before, we can work out an approximate scaling for the optical depth of LMC halo-lensing. The halo distribution is definitely less compact than the source distribution, so $\tau \propto L^2 \int \rho_l\, x\, dx$. Let a_h be the halo core radius, r_t the tidal radius (actually truncation radius), ρ_0 the halo central density, and L the distance to the LMC. Then the optical depth should scale like

$$\tau_h \propto \rho_0\, a_h^2 \left[\frac{1}{2} \log\left(1 + \frac{r_t^2}{a_h^2}\right) + \frac{\tan^{-1}(r_t/a_h)}{L/a_h} - \frac{r_t}{L} \right].$$

5.4. *Total Optical Depth*

All of the above components combine to give the total predicted optical depth for LMC/LMC self-lensing. This averaging is not completely trivial since the density of source stars is different in each population. To find an average optical depth for a set of model parameters and a set of observed fields, the optical depths for each population should be multiplied by the source density at each field location and then averaged with this weighting. Even more realistically, observational effects such as stellar crowding and observation strategy will cause the monitored source objects to differ from the underlying stellar sources and the detection efficiency of each field to vary, so additional corrections for each field should also be made. We blissfully ignore all such observational effects and assume that our model source distribution approximates the true observed source distribution with uniform source exposure and detection efficiency. Table 4 shows a summary of the optical depths for the various populations discussed above and also the averaged totals. The ranges of parameters shown in Table 3 were used. We see that for our preferred parameters a total optical depth due to known LMC stellar populations of 2.44×10^{-8} is found, with values between 0.47×10^{-8} and 7.84×10^{-8} lying in our acceptable range.

5.5. *Variation of Optical Depth across the Face of the LMC*

One potentially powerful way of distinguishing MW halo microlensing from LMC self-lensing is to compare the spatial distribution of the observed microlensing events with the predictions of LMC and halo models (Alcock et al. 1997a). For microlensing events due to an MW halo population of lenses, the lens population is uniform across the source distribution, so one expects the events to be distrib-

TABLE 4

OPTICAL DEPTHS FOR LMC SELF-LENSING

SOURCE/LENS GEOMETRY	RELATIVE WEIGHT			PREFERRED VALUES			ALLOWED RANGE (22 Fields)
	22	30	82	22	30	82	
Disk/disk	0.61	0.67	0.79	1.46	1.34	1.04	0.23–5.81
Disk/bar	0.61	0.67	0.79	0.87	0.72	0.39	0.11–4.07
Bar/disk	0.39	0.33	0.21	1.25	1.24	1.23	0.40–4.13
Bar/bar	0.39	0.33	0.21	1.37	1.36	1.33	0.32–4.00
Total bar + disk	1	1	1	2.44	2.24	1.67	0.47–7.84
(Disk + bar)/dark halo	f_M	f_M	f_M	7.75	7.73	7.18	0–22.6

NOTE.—Optical depths are in units of 10^{-8}, averaged over the 22 fields of Alcock et al. 1997a. The dark halo result is for a MACHO fraction $f_M = 1$. Note that the relative weights apply only to the the preferred set of parameters.

uted in proportion to the LMC source density times the experimental efficiency. For LMC/LMC self-lensing, both the sources and lenses are distributed like the LMC stars, so there should be a more rapid drop-off of measured optical depth at large distances from the LMC bar.

In Figure 6 we show the predicted distribution of disk/bar optical depth (times the source density in the model) as a function of right ascension and declination across the face of the LMC for our self-lensing model, employing the preferred parameters. It is clear that the optical depth drops off rapidly with radius. We note that even a few events in the regions far from the bar can rule out the LMC/LMC self-lensing hypothesis if the LMC lens population is accurately modeled as a disk/bar. Figure 7 shows the same for LMC halo lensing. Note that the halo optical depth is much less concentrated than the corresponding disk/bar result. Interestingly, there is a slight east-west asymmetry for LMC halo microlensing due to the inclination of the disk. Although such an asymmetry would be virtually impossible to detect experimentally, in principle it could be used to discriminate between LMC halo and MW halo microlensing.

Looking at Figures 6 and 7, we see that the disk/bar distribution is qualitatively distinct from the halo distribution. We can quantify this observation using a simple measure. We write $\tilde{\theta} \equiv \langle \theta_{ij} \rangle$, where θ_{ij} is the angle on the sky between the location of events i and j and the average is over all pairs. The value of $\tilde{\theta}$ is a statistic that measures the average separation of events and therefore the extent of the spatial distribution of events. It is easy to compute the experimental value, $\tilde{\theta}_{\rm obs}$, from the observed events. It is similarly easy to compute the values predicted by any given model. Since the main feature of the event distribution that should help rule out models is the central compactness, we expect that $\tilde{\theta}$ should measure whether a model can reproduce the observed event distribution in the same sense that a K-S test would. Unfortunately, the paucity of actual events may limit our ability to rule out models based upon the observed event distribution. In addition, to be useful the monitored sources must span a sufficiently wide area, since obviously we will be unable to discern any intrinsic central

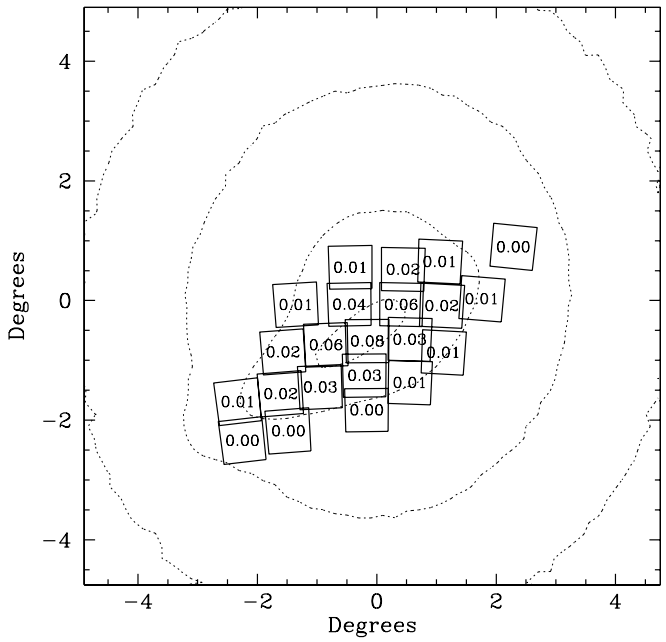

FIG. 6.—The dotted contours depict the optical depth times source number density as a function of position on the sky for LMC self-lensing for our preferred model with both disk and bar. The contours are spaced by decades. The 22 fields are overlaid along with the expected number of events using our preferred model, an exposure of 1.82×10^7 star years, and the detection efficiencies of Alcock et al. (1997a). We find a total of 0.44 expected events.

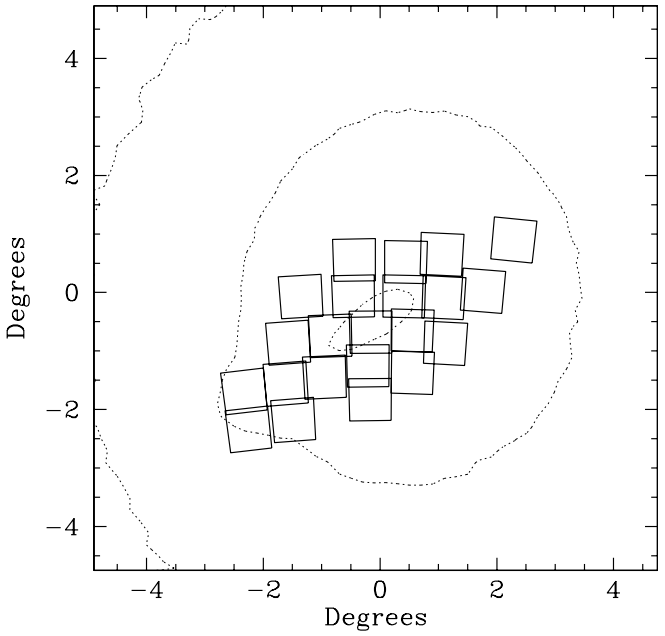

FIG. 7.—Same as Fig. 6, but for lensing by the LMC halo. Note that the distribution is much less compact than the corresponding disk/bar result; that is, the contours are much more widely spaced out.

concentration if the data sample is only a small swath of the sky.

We have computed $\tilde{\theta}$ for our models using the 22, 30, and the 82 field samples. In order to give an estimate of the allowed range of $\tilde{\theta}$, we have plotted it for numerous random parameter sets picked uniformly in parameter space. Figure 8 shows a scatterplot of τ versus $\tilde{\theta}$ for the LMC disk, LMC halo, and MW halo models. For the 22 field sample depicted in Figure 8*a*, the LMC disk/bar (*crosses*) and the LMC halo (*circles*) models are resolved in both $\tilde{\theta}$ and τ, although the experimental uncertainties on $(\tilde{\theta}_{\rm obs}, \tau_{\rm obs})$ plotted for the MACHO LMC 2 year data set do not allow them to be distinguished. We see that the selection effect of small sky coverage, in conjunction with low number statistics, does not yet allow a clear choice of model based upon the event distribution. As the extent of the fields is increased, we see superior resolution of the two distributions, as Figures 8*b* and 8*c* progressively illustrate. The 82 field sample plotted in Figure 8*c* demonstrates strong separation of the model classes in $\tilde{\theta}$. Clearly, future data with increased sky coverage and more events will be a strong discriminant between disk models and halo models. Note, however, that the plots also indicate that the LMC halo and MW halo models will probably remain degenerate.

5.6. *Other Models*

The models of Sahu (1994a, 1994b), Gould (1995), Alcock et al. (1997a), and Aubourg et al. (1999) are all contained within the framework we have explored. The main differences between the results of these different workers come from different choices of LMC model and LMC model parameter. In Table 5 we show a summary of the LMC self-lensing results of several previous workers along with the parameters they chose. We also show an approximation of their models within our framework. Note that in every case, the predicted optical depth can be found using our formulas and models and their LMC parameters. This is true even for the sophisticated N-body calculation of Weinberg (1999); substituting in his final values of parameters gives nearly the same answer as he found from his interacting and tidally disrupted model. We conclude that disagreements about the values of optical depth can be traced to disagreements about parameter choices. Workers with values of optical depth above 10^{-7} all chose parameters outside of our allowed range.

Clearly, to settle these questions, better observations of the stellar components of the LMC and its environs are needed. Direct evidence for a stellar component with an extended halo geometry would be a key to confirming a non–dark matter explanation for LMC microlensing. We now discuss some of the individual models in more detail.

Aubourg et al. (1999) have suggested an LMC model which would produce a self-lensing optical depth of $\sim 1.3 \times 10^{-7}$. If true, this would appear to solve the LMC microlensing problem. Unfortunately, there are serious objections to be raised against the stellar lensing population they employ, since there are no known tracer populations. In particular, the lenses in their model, which are ordinary stars, typically have masses 0.1–1 $M_\odot$ and the vast majority are arranged in a spherical (axis ratio ~ 0.9) isothermal distribution with velocity dispersion ~ 45 km s^{-1}. This profile and velocity are inconsistent with a multitude of tracers of the old population. Among these are the OLPV results of Bessel et al. (1986) and Hughes et al. (1991), the metal-poor giants of Olszewski (1993), and the halo-type CH stars of Cowley & Hartwick (1991). While arguments could be made that any individual tracer is not really old or does not represent the old population as a whole (Salati et al. 1999), taken together the evidence against the bulk of the mass of the LMC being in the form of an old *stellar* halo is strong. Indeed, the distribution of old clusters (Schommer et al. 1992) and the RR Lyrae star counts (Alves et al. 1999, in preparation) are particularly telling as they are almost certainly an ancient population. The Aubourg et al. model thus appears to be at odds with current observations of the LMC disk. In addition, the process they invoke for populating their spheroidal component, stochastic heating of the disk by inhomogeneities in the disk itself, has difficulties. First, the vertical diffusion coefficient they require (300 km^2 s^{-2} Gyr^{-1}) is a factor of 3 larger than the coefficient that Wielen derived for the MW, when in fact naive considerations lead one to expect a coefficient for the LMC smaller than that for the MW. Second, it is unlikely that this process would be capable of ejecting upward of 80% of the LMC disk mass into a far less centrally concentrated pseudosphere.

We can recast their model, however, in a potentially more palatable form. The MACHOs conjectured to reside in the halo of *our* Galaxy have mass of about 0.2–0.8 $M_\odot$ and are modeled in a spherical pseudoisothermal distribution. Note the striking resemblance between the conjectured MW MACHOs and the LMC lenses proposed by Aubourg et al.

TABLE 5

SUMMARY OF LMC SELF-LENSING OPTICAL DEPTHS RESULTS FOR VARIOUS GROUPS

Paper	M_{d+b} ($M_\odot$)	$M_{\rm stellar\ halo}$ ($M_\odot$)	z_d (kpc)	cos i (deg)	$\tau_{\rm paper}$	$\tau_{\rm us}$
1.....	2×10^9	0	~ 0.2	0	5×10^{-8}	5.3×10^{-8}
2.....	$\sim 1.2 \times 10^9$	0	~ 0.2	27	$\lesssim 10^{-8}$	$\sim 7.6 \times 10^{-9}$
3.....	6.8×10^9	0	0.25	30	3.2×10^{-8}	3.2×10^{-8}
4.....	Insignificant	$\sim 1.4 \times 10^{10}$	...	...	1.3×10^{-7}	1.2×10^{-7}
5.....	10^{10}	0	~ 0.4?	45	1.4×10^{-7}	1.4×10^{-7}
6.....	3×10^9	0	0.3	30	2.44×10^{-8}	2.44×10^{-8}

NOTE.—See text for more explanation. Gould's, Aubourg's, & Weinberg's results are all for a single line of sight, which overestimates the 22 field averaged optical depth by $\sim 50\%$. Sahu's model was pure bar, with no disk. Gould's optical depth was expressed in terms of the vertical velocity dispersion; we chose values of the disk mass and scale height which roughly give that dispersion. It is unclear what scale height corresponds to Weinberg's calculation, but 0.4 kpc is a reasonable estimate.

REFERENCES.—(1) Sahu 1994a; (2) Gould 1995; (3) Alcock et al. 1997a; (4) Aubourg et al. 1999; (5) Weinberg 1999; (6) this work.

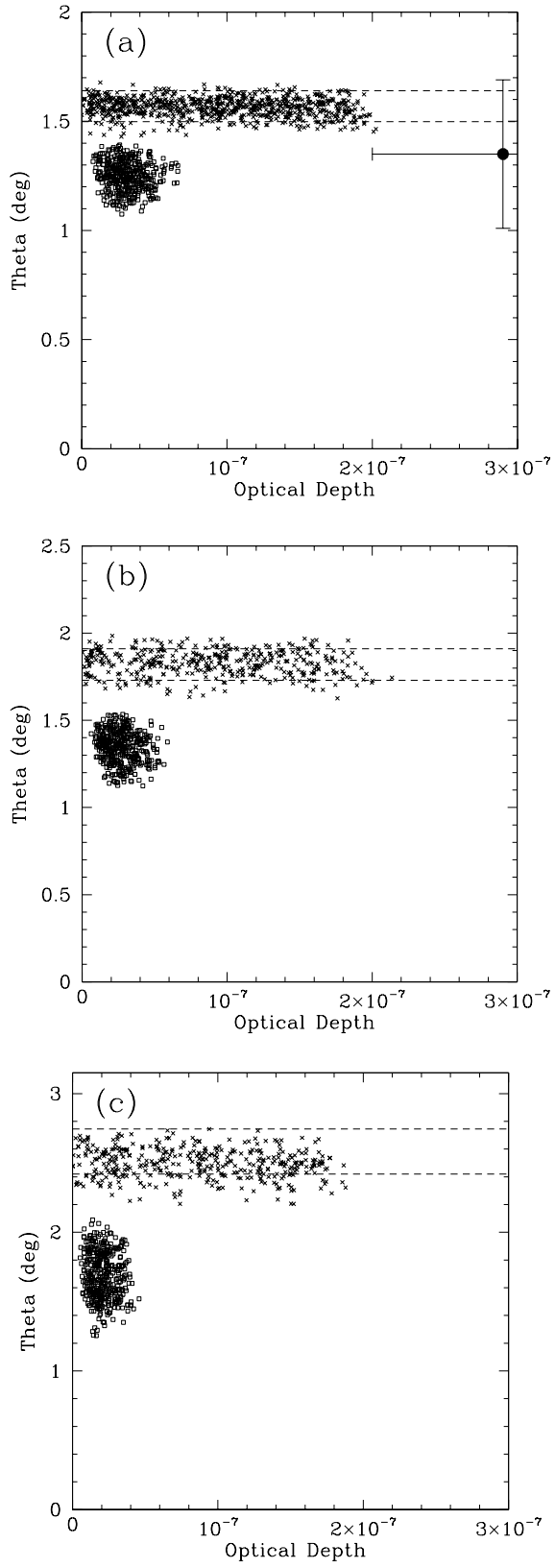

FIG. 8.—τ vs. $\tilde{\theta}$; (*a*) shows the range of τ and $\tilde{\theta}$ for the 22 field set, (*b*) shows the same for the 30 field set (appropriate for the MACHO 5 year results), and (*c*) is for the 82 field set. The open boxes are for the disk/bar, and the crosses are for the LMC halo. The points were randomly selected uniformly in parameter space within the allowed ranges. The dashed lines show the range for MW halo lensing. The point with error bars corresponds to the MACHO year 2 events (Alcock et al. 1997a). Note the increased separation of the disk/bar and halo distributions for the 82 field set.

Whether one chooses to call these undetected objects stars or MACHOs becomes a matter of semantics; we see that the Aubourg et al. model is identical in practice to a MACHO halo around the LMC. As expected, therefore, their results match our calculation for disk-halo lensing.

Very recently, Weinberg (1999) has suggested that a substantial portion (perhaps all) of the LMC microlensing might be due to LMC disk self-lensing. He models the LMC self-consistently with a sophisticated N-body code and finds that the effect of the time-varying Galactic tidal forces is to puff up the LMC disk by a factor ($\gtrsim 2$ times) without noticeably increasing the velocity dispersion. This is important since the optical depth depends strongly on scale height. Indeed, if this simulation does in fact resemble the LMC's history, then it argues against reliance upon thin-disk equilibrium solutions to the Jeans equations, à la Gould (1995). Weinberg's reported optical depth is 1.4×10^{-7}, which compares favorably with the recent estimates from the MACHO collaboration ($\sim 1.2 \times 10^{-7}$) (Alcock et al. 2000a). A few points need to be made regarding this result. First, this optical depth appears to be calculated for the line of sight to the center of the LMC instead of averaged over the observational fields. This will yield results biased upward by a factor of about 1.5. Second, Weinberg assumes an inclination of 45°. Using the more likely preferred value of 30° yields a further 15% reduction (see Weinberg's Fig. 12). Finally, the disk mass taken in his study, $10^{10}\ M_{\odot}$, appears unrealistically high. As discussed above (and matching nicely with Weinberg's own calculations in his Appendix A), the *disk* mass is unlikely to be above $5 \times 10^{9}\ M_{\odot}$. Taking all of these adjustments into account the optical depth is reduced to $\sim 4 \times 10^{-8}$, falling in line with the values calculated in this work.

Finally, we should note that Zhao (1998) has suggested that an intervening dwarf galaxy similar to the Sagittarius dwarf could be responsible for the LMC microlensing events. Searches for the RR Lyrae stars that should be contained in such a dwarf turned up negative (Alcock et al. 1997b), but Zaritsky & Lin (1997) evaded these search limits by hypothesizing the existence of either a dwarf galaxy very near the LMC itself or perhaps a tidal tail pulled from the LMC by a close encounter with the SMC. They claimed detection of a population of stars from this intervening entity. This result has been disputed in several ways by several groups. Gould (1998) and Bennett (1998) claim that the optical depth due to the Zaritsky & Lin population is insufficient to explain the microlensing results. Beaulieu & Sackett (1998) claim that the Zaritsky & Lin stars are ordinary LMC stars that are brighter due to stellar evolution and thus do not represent an intervening population. The discussion continues (Zaritsky et al. 1999; Gould 1999), and at this point, while the question has not been definitively settled, the case for an intervening dwarf looks rather weak. A variant of this suggestion (and subject to the same objections) positions the extra population well *behind* the LMC where it contributes sources with high optical depth. Such sources should have measurable velocity and magnitude biases (Zhao 1999a; Zhao, Graff, & Guhathakurta 1999).

6. DISCUSSION

We have seen that pure LMC disk/bar self-lensing models appear incapable of producing the measured optical depth of $\tau \approx 2.9 \times 10^{-7}$. Given the current state of obser-

vations of the LMC, the most likely self-lensing optical depth, based on our realistic LMC models, is an order of magnitude too small to account for the observed events. A reasonable range of self-lensing optical depths is $(0.47–7.84) \times 10^{-8}$, depending upon model parameters. We have shown that halo models can reproduce the optical depth *if* we are allowed to push the model's parameters to their extremes. We pointed out that numerous observations already limit our ability to push the parameters very far. In order to invoke a self-lensing explanation of LMC microlensing, observation of a sufficient number of stars exhibiting the characteristics of an extended halo seems crucial. Better observations of the LMC that more strongly constrain the disk scale height, inclination, disk mass, total mass, and velocity dispersion also are important as they will reduce the allowed range of optical depth. Especially important are measurements of velocity dispersion and spatial extent of old populations such as RR Lyrae.

We then discussed how consideration of the distribution of optical depth over the face of the LMC can help further distinguish between models. In particular, LMC disk/bar lensing will produce events clustered around the LMC center, while LMC halo lensing will produce a more diffuse distribution of events. We introduced a new clustering statistic, $\tilde{\theta}$, and showed that it discriminates quite well between LMC disk or bar lenses and halo lenses. The disjoint distributions of $\tilde{\theta}$ plotted in Figure 8 show that more microlensing observations distributed over the face of the LMC can be very useful in identifying LMC disk/bar self-lensing. However, distinguishing between an LMC halo and the MW halo will probably not be possible using this method.

An ingenious idea by Zhao (1999b) would take advantage of the dust layer of the LMC disk to detect LMC self-lensing. As previously noted, this layer preferentially reddens the far-side stars. In the LMC self-lensing scenario (but not for Galactic halo MACHOs) these stars have a higher optical depth compared to the nonreddened near-side stars. Thus, if LMC self-lensing is dominant, we expect the LMC event sources to be systematically reddened with respect to the field. Zhao (1999b) suggests that this reddening should be detectable in the upcoming MACHO 5 year sample with only a modest expenditure of telescope time.

Finally, we note that if the distance of some of the lenses could be directly determined, the puzzle could be solved. There are several ways to do this using microlensing fine structure, and the distance to at least one binary SMC lens has been well determined (Alcock et al. 1998; Afonso et al. 1998; Albrow et al. 1998). The interpretation of the one LMC binary lens (LMC-9) for which such a determination might have been possible was unfortunately so uncertain that a secure distance determination was not possible (Bennett et al. 1996). However, continued monitoring with good sampling should eventually allow some distances to be found using future binary events. Perhaps the most secure distance determination would come from astrometric parallax effects in microlensing. NASA's *Space Interferometry Mission*, scheduled for launch around 2006, should have the astrometric precision to make definitive parallax measurements (Paczyński 1998; Boden, Shao, & Van Buren 1998).

It has been argued that the SMC events along with LMC-9 strongly support the notion that all of the events are due to self-lensing. In this view, the next LMC binary event should definitively decide between halo- and self-lensing scenarios (Kerins & Evans 1999; Di Stefano 1999). This may not be the case. First, the SMC is *expected* to have a high self-lensing rate regardless of the nature of the LMC lenses. Coupled with the uncertain interpretation of LMC-9, the case for LMC self-lensing is poorly supported at present. In this light, the next LMC binary event alone will probably not suffice to locate the bulk of the lenses, even if it is found to be an LMC lens. First, we have seen that LMC self-lensing may well contribute of order 10%–20% of the lensing so that some self-lensing events are expected. Second, there may well be fewer binaries in the halo than the LMC, inducing a possible selection effect in favor of LMC lenses. It will probably require multiple future distance determinations to settle this matter.

Given the importance of the LMC microlensing interpretation to the dark matter question, many of the potential observational efforts described above are being attempted. We are hopeful that the interpretation of LMC microlensing will become clear within the next few years.

It is a pleasure to thank Thor Vandehei for numerous enlightening and stimulating discussions on this and related matters. We acknowledge support from the U.S. Department of Energy under grant DEFG0390ER 40546 and from Research Corporation under a Cottrell Scholar award.

REFERENCES

Afonso, C., et al. 1998, A&A, 337, L17
Albrow, M., et al. 1998, ApJ, 512, 672
Alcock, C., et al. 1997a, ApJ, 486, 697
———. 1997b, ApJ, 490, L59
———. 1997c, ApJ, 491, L11
———. 1998, ApJ, 518, 44
———. 2000a, preprint (astro-ph/0001272)
———. 2000b, preprint (astro-ph/0001435)
———. 2000c, preprint (astro-ph/0003392)
Aubourg, E., et al. 1999, A&A, 347, 850
Bahcall, J., & Tremaine, S. 1981, ApJ, 244, 805
Beaulieu, J., & Sackett, P. 1998, AJ, 116, 209
Bennett, D. 1998, ApJ, 493, L79
Bennett, D., et al. 1996, Nucl. Phys. Proc. Suppl., 51B, 152
Bessel, M. S., Freeman, K. C., & Wood, P. R. 1986, ApJ, 310, 710
Binney, J., & Tremaine, S. 1987, Galactic Dynamics (Princeton: Princeton Univ. Press)
Blackman, C. P. 1983, MNRAS, 202, 379
Boden, A., Shao, M., & Van Buren, D. 1998, ApJ, 502, 538
Bothun, G. D., & Thompson, I. B. 1988, AJ, 96, 877
Caldwell, J. A. R., & Coulson, I. M. 1986, MNRAS, 218, 223
Carignan, C., & Purton, C. 1998, ApJ, 506, 125
Cowley, A. P., & Hartwick, F. D. A. 1991, ApJ, 373, 80
de Vaucouleurs, G. 1957, AJ, 62, 69
Di Stefano, R. 1999, preprint (astro-ph/9901035)
Dottori, H., et al. 1996, ApJ, 461, 742
Dwek, et al. 1995, ApJ, 445, 716
Fields, B. D., Freese, K., & Graff, D. S. 1998, NewA, 3, 347
Freeman, K. C. 1996, in IAU Colloq. 157, Barred Galaxies, ed. R. Buta, D. A. Crocker, & B. G. Elmegreen (ASP Conf. Ser. 91; San Francisco: ASP), 1
Gates, E., Gyuk, G., & Turner, M. 1996, Phys. Rev. D, 53, 4138
Gould, A. 1995, ApJ, 441, 77
———. 1998, ApJ, 499, 728
———. 1999, ApJ, 525, 734
Gould, A., Bahcall, J., & Flynn, C. 1997, ApJ, 482, 913
Griest, K. 1991, ApJ, 366, 412
Ho, L. C., Filippenko, A. V., & Sargent, W. 1996, in IAU Colloq. 157, Barred Galaxies, ed. R. Buta, D. A. Crocker, & B. G. Elmegreen (ASP Conf. Ser. 91; San Francisco: ASP), 188
Hughes, S. M. G., Wood, P. R., & Reid, N. 1991, AJ, 101, 1304
Kenney, J. 1996, in IAU Colloq. 157, Barred Galaxies, ed. R. Buta, D. A. Crocker, & B. G. Elmegreen (ASP Conf. Ser. 91; San Francisco: ASP), 150
Kerins, E., & Evans, N. W. 1999, ApJ, 517, 734
Kim, S., et al. 1998, ApJ, 503, 674

Kinman, T. D., et al. 1991, PASP, 103, 1279
Kunkel, W. E., Demers, S., Irwin, M. J., & Albert, L. 1997, ApJ, 488, L129
Lasserre, T., et al. 1999, Proc. of Gravitational Lensing: Recent Progress and Future Goals, Boston University, July 1999, ed. T. G. Brainerd & C. S. Kochanek
Meatheringham, S. J., Dopita, M. A., Ford, H. C., & Webster, B. L. 1988, ApJ, 327, 651
Odewahn, S. C. 1996, in IAU Colloq. 157, Barred Galaxies, ed. R. Buta, D. A. Crocker, & B. G. Elmegreen (ASP Conf. Ser. 91; San Francisco: ASP), 30
Oestreicher, M., & Schmidt-Kaler, T. 1996, A&AS, 117, 303
Ohta, K. 1996, in IAU Colloq. 157, Barred Galaxies, ed. R. Buta, D. A. Crocker, & B. G. Elmegreen (ASP Conf. Ser. 91; San Francisco: ASP), 37
Olszewski, E. W. 1993, in ASP Conf. Ser. 48, The Globular Cluster-Galaxy Connection, ed. G. Smith & J. Brodie (San Francisco: ASP), 351
Olszewski, E. W., Suntzeff, N. B., & Mateo, M. 1996, ARA&A, 34, 511
Paczyński, B. 1998, ApJ 494, L23
Palanque-Delabrouille, N., et al. 1998, A&A, 332, 1
Prevot, L., Rousseau, J., & Martin, N. 1989, A&A, 225, 303
Sahu, K. C. 1994a, Nature, 370, 275
———. 1994b, PASP, 106, 942
Sahu, K. C., & Sahu, M. S. 1998, ApJ, 508, L147
Sakamoto, K., et al. 1999, ApJ, 525, 691
Salati, P., et al. 1999, A&A, 350, L57
Schommer, R. A., Olszewski, E. W., Suntzeff, N. B., & Harris, H. C. 1992, AJ, 103, 447
Udalski, A., Kubiak, M., & Szymanski, M. 1997, Acta Astron., 47, 319
Weinberg, M. 1998, in ASP Conf. Ser. 165, Third Stromlo Symp., The Galactic Halo, ed. B. K. Gibson, T. S. Axelrod, & M. E. Putman (San Francisco: ASP), 100
———. 1999, preprint (astro-ph/9905305)
Weiner, B., & Sellwood, J. 1999, ApJ, 524, 112
Welch, D. L., et al. 1987, ApJ, 321, 162
Westerlund, B. 1997, The Magellanic Clouds (Cambridge: Cambridge Univ. Press)
Wu, X. 1994, ApJ, 435, 66
Yamashita, Y. 1975, PASJ, 27, 325
Zaritsky, D., & Lin, D. N. C. 1997, AJ, 114, 2545
Zaritsky, D., Shectman, S., Thompson, I., Harris, J., & Lin, D. N. C. 1999, AJ, 117, 2268
Zhao, H. 1998, MNRAS, 294, 139
———. 1999a, ApJ, 526, 141
———. 1999b, ApJ, 527, 167
Zhao, H., Graff, D., & Guhathakurta, P. 1999, ApJ, 532, L37